J. Biochem. 2011;149(2):191–202 doi:10.1093/jb/mvq139

JB THE JOURNAL OF BIOCHEMISTRY

# A single amino acid mutation at position 170 of human parainfluenza virus type 1 fusion glycoprotein induces obvious syncytium formation and caspase-3-dependent cell death

*Received August 11, 2010; accepted October 26, 2010; published online December 24, 2010*

**Masahiro Takaguchi[1], Tadanobu Takahashi[1], Chika Hosokawa[1], Hiroo Ueyama[1], Keijo Fukushima[1], Takuya Hayakawa[1], Kazuhiko Itoh[1], Kiyoshi Ikeda[2] and Takashi Suzuki[1,*]**

[1]Department of Biochemistry, University of Shizuoka, School of Pharmaceutical Sciences and Global COE Program for Innovation in Human Health Sciences, Shizuoka 422-8526 and [2]Department of Organic Chemistry, Faculty of Pharmaceutical Sciences, Hiroshima International University, Hiroshima 737-0112, Japan

*Takashi Suzuki, Department of Biochemistry, University of Shizuoka, School of Pharmaceutical Sciences, Shizuoka 422-8526, Japan. Tel: +81 54 264 5725, Fax: +81 54 264 5725, email: suzukit@u-shizuoka-ken.ac.jp

Accession Numbers: Nucleotide sequence data reported are available in the DDBJ/EMBL/GenBank databases under the accession numbers, AB542810, AB542811 and AB542812.

**An escape mutant of human parainfluenza virus type 1 (hPIV1), which was selected by serial passage in the presence of a sialidase inhibitor, 4-*O*-thiocarbamoylmethyl-2-deoxy-2,3-didehydro-*N*-acetylneur-aminic acid (TCM-Neu5Ac2en), exhibited remarkable syncytium formation and virus-induced cell death in LLC-MK2 cells but no difference in susceptibility for the sialidase inhibitor TCM-Neu5Ac2en from that of wild-type hPIV1 strain C35 (WT). The mutant virus also had higher replication and plaque formation abilities. The mutant virus acquired two amino acid mutations, Glu to Gly at position 170 and Ala to Glu 442 in fusion (F) glycoprotein, but no mutations in haemaggulutinin-neuraminidase (HN) glycoprotein. Using cells co-expressing F and HN genes with site-specific mutagenesis, we demonstrated that a point mutation of Glu to Gly at position 170, which was estimated to be located in hPIV1 F glycoprotein heptad repeat 1, was required for obvious syncytium formation and caspase-3-dependent cell death. In contrast, wild-type F glycoprotein induced no synctium formation or cell death. The findings suggest that a single amino acid mutation of hPIV1 F glycoprotein promotes syncytium formation that is followed by caspase-3-dependent cell death.**

*Keywords*: Fusion protein/heptad repeat/human parainfluenza virus/membrane fusion/sialidase inhibitor.

*Abbreviations*: DAPI, 4, 6-diamidino-2-phenylindole dihydrochloride; F, fusion; FBS, foetal bovine serum; FFU, focus-forming units; FITC, fluorescein isothiocyanate; GRBCs, guinea pig erythrocytes; 6HB, six-helix bundles; HN, haemaggulutinin-neuraminidase; hPIV1, human parainfluenza virus type 1; hPIV3, human parainfluenza virus type 3; HR, heptad repeat; HRP, horseradish peroxidase; LLC-MK2, Lewis lung carcinoma-monkey kidney; MEM, Eagle's minimum essential medium; m.o.i., multiplicity of infection; 4-MU-Neu5Ac, 4-methylumbelliferyl-α-D-*N*-acetylneuraminic acid; PBS, phosphate-buffered saline; PI, propydium iodide; SEM, standard error of the mean; SFM, serum-free medium; TCM-Neu5Ac2en, 4-*O*-thiocarbamoylmethyl-2-deoxy-2,3-didehydro-*N*-acetylneuraminic acid; WGA, wheat germ agglutinin; WT, wild-type hPIV1 strain C35.

Human parainfluenza virus type 1 (hPIV1) belongs to the genus *Respirovirus* of the *Paramyxoviridae* family that possesses haemagglutinin-neuraminidase (HN) glycoprotein and fusion (F) glycoprotein on the viral envelope. hPIV1 recognizes terminal sialic acid of glycoconjugates on the host cell surface through HN protein and then directly initiates the fusion process into the cell surface membrane through F protein (*1*). hPIV1 often causes severe respiratory tract illness that can lead to hospitalization of infants and young children (*2*, *3*). hPIV1 infections may also cause more severe diseases, especially in the elderly and immunocompromised patients. However, there is no clinical therapy for or vaccine against hPIV1, which occasionally causes sudden death of newborns and infants (*4*). An effective strategy for prevention of hPIV1 infection is needed, especially in developed countries with a low birth rate and aging society because of the continuing decrease in the number of infants and increase in the number of elderly people, who are susceptible to hPIV1 infection. Clinical trials for hPIV1 vaccine candidates have been started with Sendai virus (*5*), and various strategies for vaccine development based on usage of recombinant hPIV1 or Sendai virus are making progress (*6*–*9*). We previously reported that 4-*O*-thiocarbamoylmethyl-2-deoxy-2,3-didehydro-*N*-acetylneuraminic acid (TCM-Neu5Ac2en) was an efficient inhibitor of hPIV1 sialidase activity and viral replication *in vitro* (*10*, *11*).

For the purpose of understanding the mechanism of resistance of hPIV1 against the sialidase inhibitor, we obtained an escape mutant virus that had efficient capability to replicate in the presence of

TCM-Neu5Ac2en. Although sialidase inhibitors generally target active site on HN glycoprotein, the mutant virus had two amino acid changes in F glycoprotein but not HN glycoprotein. The escape mutant virus showed a high level of fusion activity, high level of ability to replicate and strong cell death induction in comparison with those of wild-type hPIV1 C35 strain (WT). Both the HN and F glycoproteins of hPIVs have been shown to be involved in effective membrane fusion and viral replication (*12*). In the binding to and entry into cells of paramyxoviruses, HN glycoprotein has been shown to be essential for the F protein-mediated fusion process (*13–17*). However, a major determinant of hPIV1 F glycoprotein that participates in the promotion of membrane fusion is still unknown.

In the present study, we demonstrated by using site-specific mutagenesis and cells co-transfected with HN and F genes that a single amino acid mutation at position 170 of hPIV1 F glycoprotein induced obvious syncytium formation and caspase-3-dependent cell death.

## Materials and Methods

### *Cells and viruses*

Lewis lung carcinoma-monkey kidney (LLC-MK2) cells were maintained in Eagle's minimum essential medium (MEM) supplemented with heat-inactivated 5% foetal bovine serum (FBS). The hPIV1 strain C35 (ATCC-VR94) was obtained from the American Type Culture Collection (Manassas, VA, USA). To isolate escape mutant viruses, serial passages of WT were performed in the presence of TCM-Neu5Ac2en. Confluent monolayers of LLC-MK2 cells in a 24-well plate were inoculated with WT suspension in a serum-free medium (SFM; Hybridoma-SFM, Invitrogen Corp., Carlsbad, CA, USA) at a multiplicity of infection (m.o.i.) of 0.01 for 1 h at room temperature. In the initial passage, the cells were cultured at 34°C for 48 h in MEM (0.4 ml/well) containing 3 mM TCM-Neu5Ac2en, a concentration that has been shown to completely inhibit replication of WT (*10*), 0.1% bovine serum albumin and acetylated trypsin (1 μg/ml). In later passages the culture medium (0.2 ml), harvested at 48 h post-infection, was added to confluent monolayers of intact LLC-MK2 cells in a 24-well plate and the cells were cultured at 34°C for 48 h in MEM (0.4 ml/well) containing 300 μM TCM-Neu5Ac2en, which has been shown to completely inhibit viral sialidase activity and to cause >50% inhibition of WT replication (*10*), 0.1% bovine serum albumin and acetylated trypsin (1 μg/ml). The serial passages were performed twelve times every 48 h in the presence of TCM-Neu5Ac2en (300 μM) until detection of viral haemagglutination activity in culture media. Escape mutant viruses were isolated from the culture media by a plaque assay with SFM.

### *Plasmid construction of HN and F genes*

Each viral RNA was isolated from virus particles with TRIzol reagent (Invitrogen Corp., Carlsbad, CA, USA) according to the manufacturer's instructions. Full-length cDNAs of the HN and F genes were amplified by using a TaKaRa RNA PCR$^{TM}$ kit (AMV) ver. 3.0 (TaKaRa Bio Inc., Shiga, Japan). The HN gene was subcloned into the site between *EcoR* I and *Xho* I of the pCAGGS/MCS vector. F genes of WT and the mutant were subcloned into the pGEM-T Easy vector (Promega, Madison, WI, USA) to generate pGEM-F vectors. The fragment of each F gene from pGEM-F vectors treated with *EcoR* I was inserted into the *EcoR* I site of the pCAGGS/MCS vector to generate pCAGGS-F vectors. To determine the amino acid residues associated with fusion activity, small fragments and large fragments from *Mun* I digestion of pCAGGS-F vectors of WT and the mutant (F nucleotide positions at 176 and 1254) were ligated into each counterpart.

### *Cell–Cell fusion assay*

For quantification of cell–cell fusion of hPIV1-infected cells, confluent monolayers of LLC-MK2 cells in 6-well plates were infected with each virus diluted by SFM at m.o.i. of 1 for 30 min at room temperature. The plates were incubated at 37°C until the syncytium formation was visualized in culture of SFM (1.5 ml/well) containing acetylated trypsin (1 μg/ml). The virus-infected monolayers were fixed with 1 ml of cold methanol for 5 min and then were treated with 1 ml of Carrazzi's haematoxylin solution phosphate-buffered saline (PBS; 1 : 1, vol/vol) (Wako Pure Chemical Industries Ltd, Osaka, Japan) in order to visualize the nuclei. Fusion efficiency (%) of the cells infected were calculated as a percentage of the number of nuclei in fusion cells relative to the sum total of nuclei in all cells under 10 optical observations at a magnification of 100.

For quantification of cell–cell fusion of transfected cells with HN and F genes, LLC-MK2 cells were seeded in 24-well plates at $4 \times 10^4$ cells/well. After being cultured for 24 h, the cells were co-transfected with 1 μg of pCAGGS-HN and F or the mutant vectors using the transfection reagent TransIT-293 (Mirus, Madison, WI, USA) according to the manufacturer's instructions. As a negative control, pCAGGS/MCS vector was used instead of pCAGGS-F vector. After incubation at 37°C for 6 h, the co-transfected cells were washed with PBS and then replaced with 0.5 ml of SFM containing acetylated trypsin (1 μg/ml). After incubation at 37°C for 60 h, the cells were fixed with 0.5 ml of cold methanol for 5 min and then treated with 0.5 ml of Carrazzi's Haematoxylin Solution-PBS (1 : 1; vol/vol) in order to visualize the nuclei. Fusion efficiency (%) of transfected cells was calculated as a percentage of the number of nuclei in fusion cells relative to the sum total of nuclei in all cells under six optical observations at a magnification of 100.

### *Confocal fluorescence microscopy*

hPIV1-infected cells and cells co-transfected with HN and F genes were observed by fluorescence staining to visualize cell–cell fusion. LLC-MK2 cells were cultured on 3-well glass coverslips at $6 \times 10^4$ cells/well or $1 \times 10^4$ cells/well. The cells ($6 \times 10^4$ cells/well) were infected with hPIV1 (1 m.o.i.). The other cells were co-transfected with 0.5 μg of pCAGGS-HN and F or the mutant vectors. The cells were incubated at 37°C for 40 and 48 h, respectively. After fixation with cold methanol, the cells were incubated with rabbit anti-hPIV1 polyclonal antibody and biotinylated wheat germ agglutinin (WGA) (Seikagaku Kogyo Company Ltd, Tokyo, Japan) at 4°C for 2 h, followed by decoration with fluorescein isothiocyanate (FITC)-conjugated goat anti-rabbit IgG (Invitrogen/Molecular Probes, Carlsbad, CA, USA). Nuclei were stained with 4, 6-diamidino-2--phenylindole dihydrochloride (DAPI) (Dojindo Laboratories, Kumamoto, Japan). The hPIV1-infected cells were incubated with Cy5-streptavidin (GE Healthcare, Waukesha, WI, USA) at 4°C for 2 h, and the co-transfected cells were incubated with Cy3-streptavidin (Sigma-Aldrich Corp., St Louis, MO, USA) at 4°C for 2 h. The cells were washed three times with PBS on each step. The cellular compartments were imaged by confocal microscopy (LSM 510 meta; Carl Zeiss Inc., Thornwood, NY, USA).

### *Haemolysis assay*

Guinea pig erythrocytes (GRBCs) were resuspended at a concentration of 1% (vol/vol) in cold PBS. After 30 μl of RBCs had been mixed with 30 μl of virus suspension, the mixtures were incubated on ice for 20 min with periodic shaking at intervals of 10 min to allow the virus to bind to GRBCs, followed by incubation at 37°C with periodic shaking at intervals of 15 min to facilitate the fusion process between virus and GRBCs. Non-haemolyzed GRBCs were removed by centrifugation at 900×*g* for 1 min at 4°C. The concentrations of haemoglobin in 50 μl of the supernatants were determined by measuring the absorbance at 415 nm (*18*). To achieve complete haemolysis as a positive control, super pure water was added to GRBCs instead of virus suspension. The haemolysis induced by viruses was expressed as a percentage relative to the absorbance of each sample haemolyzed with super pure water.

### *Focus-forming assay*

LLC-MK2 cells in 12-well plates were inoculated with 0.5 ml of serial dilutions of virus suspension or the supernatant at room temperature for 30 min. Monolayers of the cells were overlaid with 2 ml of a solution of SFM containing acetylated trypsin (3 μg/ml) and 1.2% microcrystalline cellulose Avicel (FMC Corporation, Philadelphia,

PA, USA) at 37°C for 36 to 42 h (*19*). The cells were fixed with 800 µl of cold methanol for 5 min and reacted with rabbit anti-hPIV1 antibody at room temperature for 30 min and then with horseradish peroxidase (HRP)-conjugated Protein A at room temperature for 30 min. Focus-forming units (FFU) as infectious virus titres were determined from the immunostained foci developed as described previously (*20*).

### Plaque assay

Confluent monolayers of LLC-MK2 cells were inoculated with log dilutions of the virus in SFM at room temperature for 30 min. The cell monolayers were overlaid with a solution of MEM containing acetylated trypsin (3 µg/ml) and 1% agarose. The monolayers were incubated at 37°C for 9 days. The plaques were fixed with an ethanol–acetic acid (5 : 1; vol/vol) solution and were immunostained as described in the focus forming assay (*20*). Then the cells were treated with 0.5% amide black in an ethanol-acetic acid-water (45 : 10 : 45; vol/vol/vol) solution to confirm plaque formation.

### Virus penetration assay

Virus penetration was determined by a slightly modified assay previously described (*21*). Confluent monolayers of LLC-MK2 cells on 6-well culture plates were inoculated with approximately 300 FFU/well of virus in cold SFM on ice for 1 h. Then the plates were incubated at 37°C for 0, 7 and 15 min. Viruses that had not penetrated into the cells were inactivated by treatment of cells with 1.5 ml/well of citrate buffer (40 mM sodium citrate, 10 mM KCl, 135 mM NaCl, pH 3.0) at room temperature for 2 min. After washing with PBS, the cells were overlaid with 4 ml of SFM containing 1.2% Avicel and acetylated trypsin (3 µg/ml) and incubated at 37°C for 40 h. Virus infectivities were determined as FFU by focus-forming assay. Penetration rate was expressed as a percentage relative to the number of FFU in PBS that was used instead of citrate buffer as a control.

### Virus receptor binding assay

Confluent monolayers of LLC-MK2 cells on 96-well culture plates were washed with PBS and were treated with 50 µl of SFM or SFM containing *Arthrobactor ureafaciens* sialidase (10 mU/ml) at 37°C for 1 h. The cells were fixed with 50 µl of cold methanol for 5 min and washed three times with PBS. The cells were blocked with 200 µl of PBS containing 0.5% lipid-free bovine serum albumin at 4°C for 12 h as described previously (*1*). After the blocking, the cells were incubated with 50 µl of each virus suspension (serial 2-fold dilution from 2 to 128 HAU) in blocking solution on ice for 2 h. Unbound viruses were removed by washing with PBS containing 0.01% Tween-20. The bound virions on the cells were reacted with rabbit anti-hPIV1 polyclonal antibody followed by HRP-conjugated Protein A at 4°C for 2 h. The bound virions on the cells were determined by measuring the absorbance at 490 nm with *O*-phenylenediamine as a substrate as described previously (*22*). Values of the binding curve were obtained in three independent experiments. $K_d$ and $B_{max}$ were analysed by non-linear regression of the saturation curve using the Program GraphPad Prism 5 (GraphPad Software Inc., San Diego, CA, USA).

### Sialidase activity assay

Sialidase activities of hPIV1 strains were measured by using 4-methylumbelliferyl-α-D-*N*-acetylneuraminic acid (4-MU-Neu5Ac) as a substrate. Four microliters of each virus suspension in 100 mM acetate buffer (pH 4.6) was reacted with 1 µl of 4-MU-Neu5Ac (0.4–8.0 mM) at 37°C for 30 min. The reaction was stopped with 100 µl of 500 mM carbonate buffer (pH 10.2). The fluorescent intensities of the released 4-methylumbelliferone were determined by using a Wallac 1420 ARVOsx Multilabel Counter (PerkinElmer Life Science, Boston, MA, USA) with excitation at 355 nm and emission at 460 nm. The values of each time or concentration point were measured in triplicate. $K_m$ and $V_{max}$ were calculated by using a Hanes–Woolf plot.

### Sialidase inhibition assay by TCM-Neu5Ac2en

Each virus suspension was used as described in the section of sialidase activity assay. Four microlitres of each virus suspension was mixed with 1 µl of TCM-Neu5Ac2en (serial 2-fold dilution with distilled water from 10 to $9.8 \times 10^{-3}$ mM), and incubated on ice for 1 h. After incubation, sialidase activity of each virus was measured in the same way as that described in the section of sialidase activity assay.

### Inhibition of virus replication by TCM-Neu5Ac2en

Confluent monolayers of LLC-MK2 cells on 96-well culture plates were infected with each virus at m.o.i. of $1.0 \times 10^{-2}$ FFU/cell in 0.1 ml of SFM containing acetylated trypsin (1 µg/ml) and 300 or 1000 µM TCM-Neu5Ac2en. As a control, PBS was used instead of TCM-Neu5Ac2en solution. After incubation at room temperature for 30 min, the cells were incubated at 37°C for 36 h. Infectious virus titers in each supernatant were determined by focus-forming assay on LLC-MK2 cells.

### Titres of progeny viruses released from cells

Confluent monolayers of LLC-MK2 cells on 24-well culture plates were inoculated with 250 µl of each virus suspension in SFM at m.o.i. of $2.0 \times 10^{-3}$ (FFU/cell). After incubation at room temperature for 30 min, the inocula were removed and the cells were washed once with PBS. After addition of 1 ml of SFM containing acetylated trypsin (1 µg/ml), the cultured supernatants were collected at 8, 10, 12, 24, 36 and 50 h post-infection. Infectious progeny virus titers in each supernatant were determined by focus-forming assay on LLC-MK2 cells.

### Detection of virus-induced cell death and activated caspase-3

Quantification of cell cytotoxicity was performed by flow cytometric analysis. Confluent monolayers of LLC-MK2 cells on 24-well culture plates were inoculated with 250 µl of each virus suspension in SFM at m.o.i. of 4 (FFU/cell) at room temperature for 30 min. After washing once with PBS, the cells were cultured in 1 ml of SFM containing acetylated trypsin (1 µg/ml). The supernatants were collected at 24 and 50 h post-infection. Infectious progeny virus titers in each supernatant were determined by focus-forming assay. The virus-infected cells were harvested by treatment with 100 µl of 0.125% trypsin-PBS for measurement of virus-induced cell death and caspase-3 activation. After fixation with 70% ethanol, DNA fragmentation in the cells was detected by treatment with propydium iodide (1 µg/ml) (PI; Dojindo, Kumamoto, Japan) in hypotonic lysis buffer (0.1% sodium citrate, 0.1% Triton X-100) containing DNase free RNase A (100 µg/ml) (Novagen, Darmstadt, Germany) on ice for 1 h. Detection of caspase-3 activity was measured using the NucView™ 488 caspase-3 Assay Kit for Live cells (Biotium Inc., Hayward, CA, USA). The substrate of the caspase-3 assay kit is cleaved to a fluorogenic DNA dye and a DEVD substrate moiety by caspase-3 activity in cells. Then the DNA dye migrates to the cell nucleus to stain the nucleus bright green. Briefly, after 100 µl of MEM containing 5% FBS was added to cells detached by trypsin, 50 µl of obtained cells was suspended in 150 µl of PBS. The cell suspension was treated with 2 µl of NucView™ 488 Caspase-3 substrate stock solution at room temperature for 25 min and then fixed with 4% paraformaldehyde. As an indication of cell death, sub-G1 fraction (%) and caspase-3 activity (%) were analysed by using a BD FACS Canto II flow cytometer (BD Biosciences, San Jose, CA, USA). At least $1.0 \times 10^4$ cells were used for analysis of each sample.

### Detection of cell death and caspase-3 activation in transfected cells

LLC-MK2 cells were transfected with 1 µg of pCAGGS-HN and F or the mutant vectors using the transfection reagent TransIT-293. After incubation at 37°C for 6 h, the cells were washed with PBS and then replaced with 1 ml of SFM containing acetylated trypsin (1 µg/ml). After incubation at 37°C for 72 h, the cells were stained with 200 µl of MEM containing 5% FBS, 2 µM NucView™ 488 caspase-3 Assay Kit for live cells, PI (2 µg/ml) and DAPI (2 µg/ml). Cell death and caspase-3 activation were determined by observation using a fluorescent microscope (OLYMPUS IX71, Olympus, Tokyo, Japan). Treatment of the transfected cells with Z-VAD-FMK (R&D Systems Inc., Minneapolis, MN, USA) was performed by exchanging SFM containing 50 µM Z-VAD-FMK every 24 h from 6 h pre-transfection to 72 h post-transfection. As a control, a quantity of DMSO equal to Z-VAD-FMK was used.

### *Statistical analysis*

Results are shown as averages. Student's t-test and Mann-Whitney's U-test were used to perform statistical analyses.

## Results

### *Escape mutant virus selected by serial passage in the presence of a sialidase inhibitor promotes cell–cell fusion*

An escape mutant virus of hPIV1 that was selected by serial passage in the presence of TCM-Neu5Ac2en acquired two amino acid mutations, Glu to Gly at position 170 and Ala to Glu 442, in F glycoprotein but no mutations in HN glycoprotein (Table I). We measured syncytium formation and haemolytic activity to compare fusion activity of the mutant virus with that of WT. Obvious syncytium formation was observed in LLC-MK2 cells infected with the mutant virus, but cells infected with WT showed no syncytium formation (Fig. 1A and B). Similar syncytium formation was also observed in HEp-2 cells infected with the mutant but not with WT (Supplementary Fig. S1). To elucidate each cellular compartment in the virus-infected cells, nuclei, cellular membrane and viral antigens were stained by DAPI, biotinylated WGA and rabbit anti-hPIV1 polyclonal antibody, respectively. This fluorescent detection also showed that the mutant virus but not WT remarkably induced syncytium formation (Fig. 1C).

Haemolytic activity of the mutant virus was also significantly increased in amount of the virus (HAU activity) (Fig. 1D) or incubation time-dependent manner (Fig. 1E), but WT showed little haemolytic activity under the same conditions.

**Table I. Nucleotide and amino acid comparison of F glycoprotein between WT and the mutant virus.**

| | Position | | | |
|---|---|---|---|---|
| | Nucleotide | | Amino acid | |
| | 509 | 1325 | 170 | 442 |
| Virus | | | | |
| WT | A | C | Glu | Ala |
| Mutant | G | A | Gly | Glu |

### *The mutant virus does not have resistance against the sialidase inhibitor*

To investigate the multiplication mechanism of the mutant in the presence of the sialidase inhibitor TCM-Neu5Ac2en, sialidase activity and replication ability of the mutant virus and WT were examined in the presence of TCM-Neu5Ac2en. Sialidase activities of the mutant virus and WT were inhibited in a similar manner by TCM-Neu5Ac2en (Fig. 2A). In contrast, progeny virus production of the mutant in

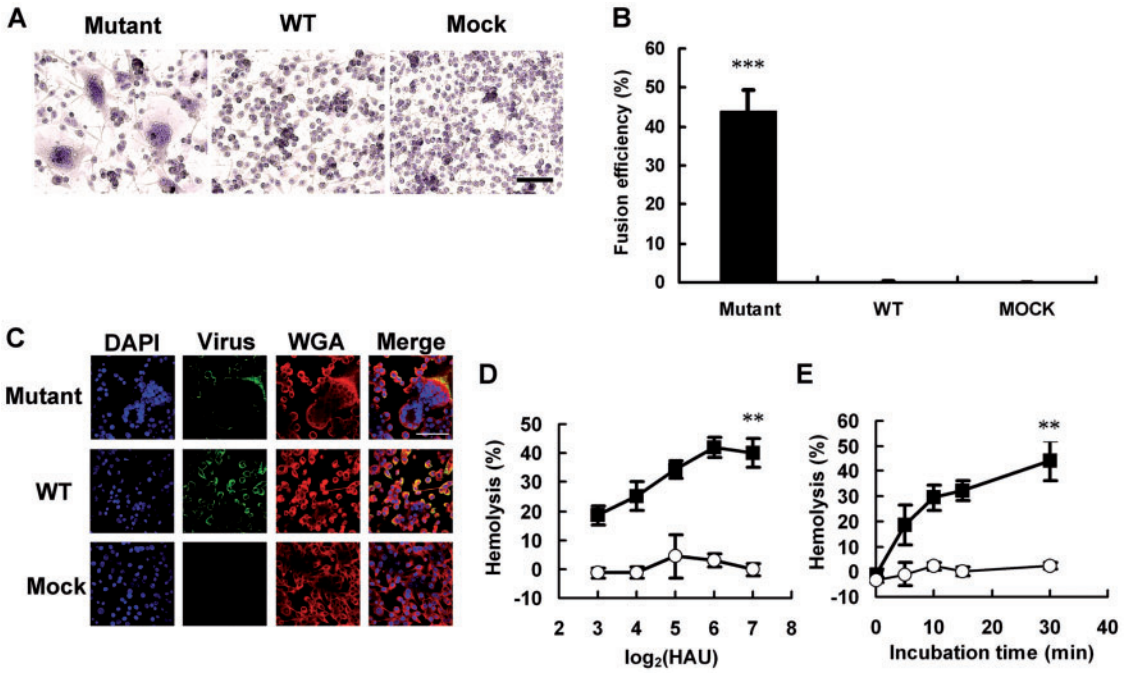


**Fig. 1 Syncytium formation and fusion activity of the mutant virus.** (A) LLC-MK2 cells were infected with each virus at m.o.i. of 1 and fixed with methanol at 48 h post-infection. Syncytium formation was determined by microscopic images of haematoxylin-stained cells. Scale bar is 100 μm. (B) Fusion efficiency (%) of the cells infected as in (A) were calculated as a percentage of the number of nuclei in fusion cells relative to the sum total of nuclei in all cells under 10 optical observations at a magnification of 100. (C) LLC-MK2 cells were infected with each virus at m.o.i. of 1 and cultured at 37°C for 40 h. Nucleus (blue), virus antigen (green) and cells (red) were stained with DAPI, rabbit anti-hPIV1 polyclonal antibody and WGA lectin, respectively. Scale bar is 100 μm. (D) 1% (v/v) GRBCs were incubated with each virus suspension (8—128 HAU) on ice for 20 min followed by incubation at 37°C for 15 min. Haemolysis (%) of the erythrocytes depending on virus titres was determined by measuring the absorbance at 415 nm as described in section 'Materials and Methods' section. (E) GRBCs were incubated with each virus suspension (128 HAU) on ice for 20 min. Haemolysis (%) of the erythrocytes depending on incubation time (0–30 min) was determined. The values are means and standard deviations of triplicate experiments. Mutant virus, closed squares; WT, open circles. $^{**}P<0.01$ and $^{***}P<0.001$.

LLC-MK2 cells was increased to a level ~10-fold higher than that of WT, regardless of the presence or absence of TCM-Neu5Ac2en (Fig. 2B).

### *The kinetic parameter $V_{max}$ of the mutant virus sialidase were lower than those of WT*

In the case of mumps virus (*23*, *24*) and human parainfluenza virus type 3 (hPIV3) (*25*), which belong to the genus *Rubulavirus* and the genus *Respirovirus*, respectively, it has been shown that enhancement of their fusogenic activity was associated with lower sialidase activity. The sialidase activity of the mutant virus per ng of viral protein was ~60% of WT (Fig. 3A). To clarify the relationship between fusion activity and sialidase activity in WT and the mutant virus, kinetics of the viral sialidases were measured with 4-MU-Neu5Ac (Fig. 3B) and the parameters ($K_m$ and $V_{max}$) were determined from the Hanes–Woolf plot (Fig. 3C). $K_m$ values were not significantly different between WT and the mutant virus. In contrast, $V_{max}$ values showed a significant difference, the $V_{max}$ value of the mutant virus being approximately two-times lower than that of WT (Table II).

The receptor-binding activity of each virus was evaluated by a cell binding assay. The binding parameters ($K_d$ and $B_{max}$) were analysed from the saturation curve (Fig. 3D). The values of $K_d$ *and* $B_{max}$ were not significantly different between WT and the mutant virus (Table III).

### *Growth ability of the mutant virus is higher than that of WT*

We compared the viral growth ability by using tissue culture supernatants from LLC-MK2 cells infected with a low m.o.i. of each virus. Virus titers in the supernatants at selected time points were determined by focus-forming assay. The replication of the mutant was 10-times higher than that of WT until 36 h post-infection (Fig. 4A). Additionally, to assess fusion activity of each virus in terms of virus–cell fusion, penetration assay was performed in LLC-MK2 cells. The mutant virus penetrated ~2- to 3-fold more quickly into cells than did WT at 7 and 15 min of incubation immediately after viral attachment to the cell surface on ice (Fig. 4B).

### *Amino acid change at position 170 in F glycoprotein increases fusion activity*

To identify amino acid determinants of the mutant F glycoprotein that trigger the increased fusion activity, pCAGGS-F expression plasmids of WT or three mutants F of glycoprotein genes with a single amino acid change at position 170 (from E to G : E170G) or 442 (from A to E : A442E) or changes in two amino acids at positions 170 and 442 (E170G/A442E) were co-transfected with the WT HN expression vector into LLC-MK2 cells. F glycoprotein expression on the cell surface was quantified by flow cytometry analysis (Supplementary Table S1). Cell surface expression of E170G and A442E was equivalent to that of WT. However, the expression of E170G/A442E was only

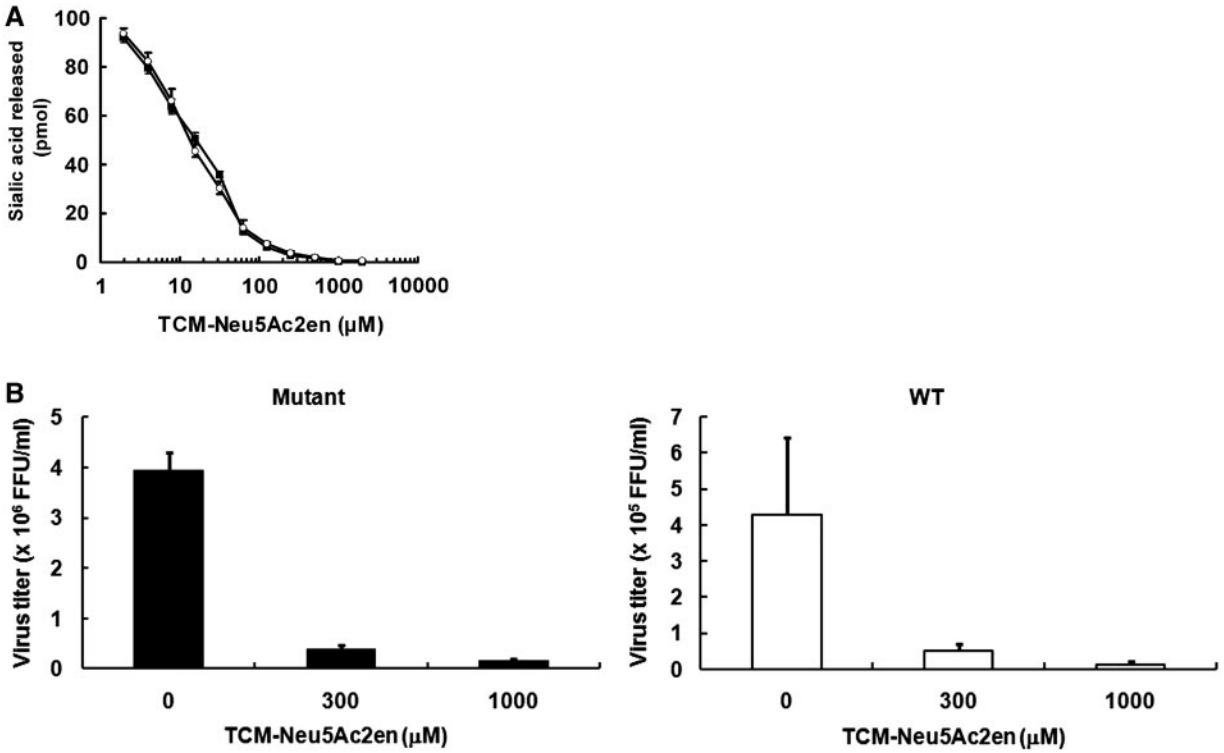


**Fig. 2 Sensitivity of the mutant virus sialidase activity and replication to TCM-Neu5Ac2en.** (A) Sialidase inhibition of the mutant virus and WT by TCM-Neu5Ac2en was determined as described in 'Materials and Merthods' section. Each virus was incubated with different concentrations of TCM-Neu5Ac2en ($2–2 \times 10^3$ μM) on ice for 1 h. Sialidase activities of the mutant virus (closed squares) and WT (open circles) were measured by using 4-MU-Neu5Ac as a substrate. (B) Inhibition of mutant virus (closed column) and WT (open column) replication in LLC-MK2 cells by TCM-Neu5Ac2en was measured as described in 'Materials and Methods' section. Progeny virus production from LLC-MK2 cells treated with 0, 300 or 1000 μM was depicted into the virus titer (FFU/ml). The values are means and standard deviations of triplicate experiments.

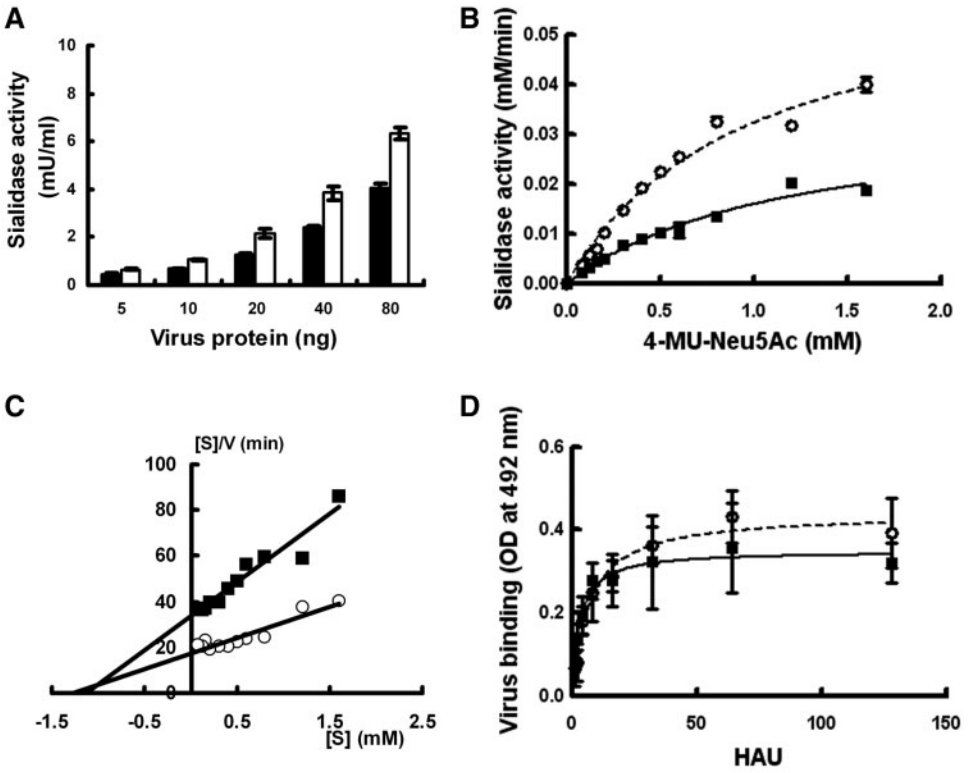


**Fig. 3 Comparison of sialidase activity and receptor binding activity of the mutant virus and WT.** (A) Sialidase activities of the mutant virus (closed column) and WT (open column) were measured with different viral protein amounts as described in 'Materials and Methods' section. (B) Sialidase activity (mU/min) of each virus was measured with various concentrations of 4-MU-Neu5Ac (0–1.6 mM). (C) Kinetics of each sialidase activity was analysed by a Hanes–Woolf plot. [S], substrate concentration; V, emzymatic velocity. (D) Binding of the mutant virus (closed squares) and WT (open circles) to LLC-MK2 cells fixed with cold methanol was determined by enzyme immunoassay with rabbit anti-hPIV1 polyclonal antibody and HRP-conjugated Protein A as described in 'Materials and Methods' section. The values are means and standard deviations of triplicate experiments.

**Table II. Kinetic parameters of viral sialidase activities.**

| Virus | $K_m$ (mM) ± SEM | $V_{max}$ (mM/mim) ± SEM |
|---|---|---|
| WT | 1.289 ± 0.029 | 0.073 ± 0.001 |
| Mutant | 1.122 ± 0.048 | 0.033 ± 0.001[a] |

[a] $P < 0.01$.

**Table III. Kinetic parameters of viral receptor binding activities.**

| Virus | $K_d$ (μg/ml)* ± SEM | $B^*_{max}$ ± SEM |
|---|---|---|
| WT | 8.645 ± 2.982 | 0.492 ± 0.115 |
| Mutant | 7.241 ± 1.862 | 0.310 ± 0.113 |

*$K_d$ and $B_{max}$ were analysed by nonlinear regression of the saturation curve using Program GraphPad Prism 5.

half of that of WT. Many syncytial cells were observed by transfection with the F gene having a single amino acid change at position 170 (E170G) or changes in two amino acids at positions 170 and 442 (E170G/A442E), while expression of A442E as well as WT exhibited low syncytium formation (Fig. 5A and B). The fusion efficiency was increased approximately six times by transfection with E170G or E170G/A442E compared to that of WT or A442E (Fig. 5C). Transfection with the F gene alone did not induce syncytium formation in LLC-MK2 cells (data not shown), indicating that HN glycoprotein contributes to activation of the fusion process (*13–17*). Syncytium formation was also observed in HEp-2 cells transfected with E170G or E170G/A442E but not with A442E or WT (Supplementary Fig. S2), suggesting that this increased fusion activity was independent of cell type. While, Bousse *et al.* (*26*) had shown that coexpression of wild-type F and HN glycoproteins of hPIV1 resulted in extensive syncytium formation. They used HeLa T4+ cells infected with recombinant vaccinia virus which express T7 RNA polymerase for expression of F and HN glycoproteins. The experimental conditions may have enhanced the syncytium formation. The three-dimensional structure of F glycoprotein from hPIV3 but not that from hPIV1 had been determined. We therefore estimated the location of the amino acid at position 170 in hPIV1 F glycoprotein from the structure of hPIV3 F glycoprotein. F glycoprotein contains two heptad repeat (HR) domains, which are important for fusion activity. The HR1 and HR2 domains are located in the downstream region of the fusion peptide and next to the transmembrane domain, respectively. HR1 and HR2 form six-helix bundles (6HB) in post-fusion. The amino acid residue at position 170, which is involved in enhancement of

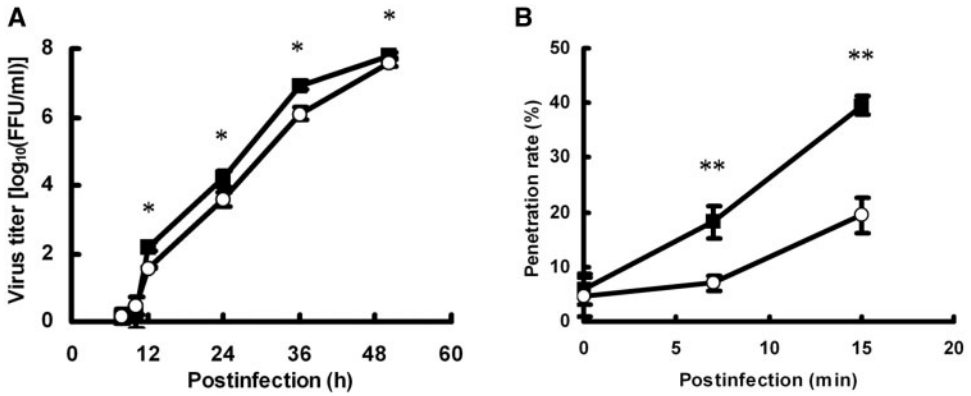


**Fig. 4 Replication and penetration rate of the mutant virus.** (A) LLC-MK2 cells were inoculated with the mutant virus (closed squares) and WT (open circles) at $2.0 \times 10^{-3}$ m.o.i. and cultured in the presence of acetylated trypsin (1 μg/ml) at 37°C. Progeny virus titers in the supernatant at 8, 10, 12, 24, 36 and 50 h post-infection were measured by focus forming assay. (B) LLC-MK2 cells in 6-well plates were inoculated with each virus ($3.0 \times 10^2$ FFU/well), and the number of foci was counted as described in 'Materials and Methods' section. Penetration rates of the mutant virus (closed squares) and WT (open circles) were expressed as a percentage relative to the number of each FFU in PBS, which was used instead of citrate buffer as a control. Data from triplicate experiments were analysed. $^*P < 0.05$ and $^{**}P < 0.01$.

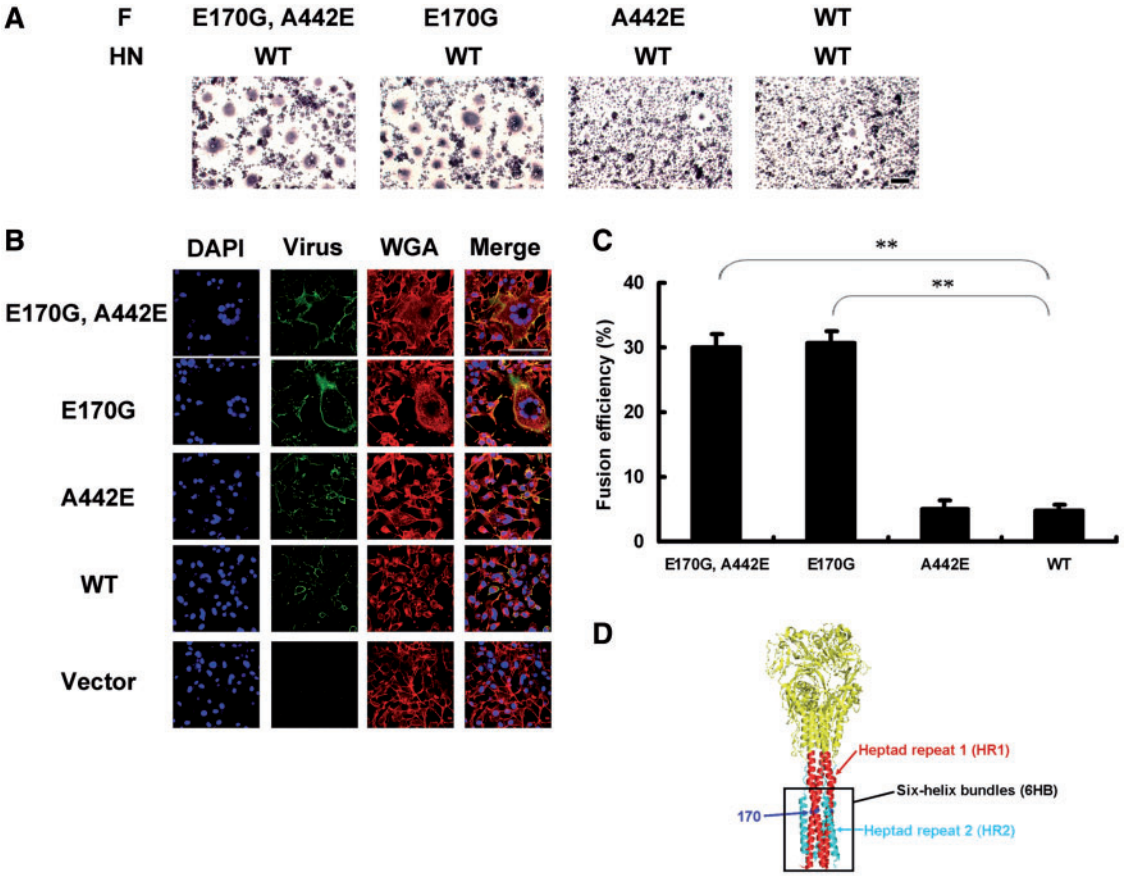


**Fig. 5 Identification of a single amino acid mutation in F glycoprotein involved in remarkable fusion activity.** (A) Fusion activity of LLC-MK2 cells that had been co-transfected with both wild-type HN gene and wild-type or mutated F gene was examined under a microscope with haematoxylin staining at 48 h post-transfection as described in 'Materials and Methods' section. Scale bar is 100 μm. (B) LLC-MK2 cells co-transfected as in (A) were treated with DAPI, rabbit anti-hPIV1 polyclonal antibody, and biotinylated WGA lectin, respectively. Nucleus (blue), viral proteins (green), and cells (red) were imaged by confocal microscopy with FITC-conjugated goat anti-rabbit IgG and Cy5-streptavidin for detection of multinuclear cells. Scale bar is 100 μm. (C) Fusion efficiency (%) of transfected cells in (A) was calculated as a percentage of the number of nuclei in fusion cells relative to the sum total of nuclei in all cells under six optical observations at a magnification of 100. (D) Location of the amino acid residue at position 170 (blue) of hPIV1 F glycoprotein was estimated from the three-dimensional structure of of hPIV3 F glycoprotein (PDB ID, 1ztm). Red, HR1; Cyan, HR2. $^{**}P < 0.01$.

fusion activity, existed in HR1 according to the three-dimensional structure of F glycoprotein of hPIV3 (Fig. 5D) (*27*). Additionally, functional characterization of canine distemper virus F proteins and measles virus attachment proteins chimeras showed that the amino acid residues identified in either glycoproteins contributed interdependently to the formation of functional interactions (*28*). The report supports that the mutation of E170G likely constitutes the low $V_{max}$ value of the mutant virus sialidase.

### *The mutant promotes virus-induced cell death in LLC-MK2 cells*

After inoculation with each virus, a cytopathic effect was strikingly observed in the mutant virus-infected cells (data not shown). To compare cytotoxicity of each virus in LLC-MK2 cells, measurement of dead cell ratio and caspase-3 activation in infected cells at a high m.o.i. was performed by flow cytometric analysis. To detect the dead cell ratio in infected cells, cells were stained with PI at 24 and 50 h post-infection. The sub-G1 population was induced up to ~60% in the mutant-infected cells at 50 h post-infection (Fig. 6A and B). On the other hand, the sub-G1 population was slightly induced in WT-infected cells at 50 h post-infection but was similar to that in Mock treatment. We then treated infected cells with the caspase-3 substrate at 24 and 50 h post-infection to assess virus-induced caspase-3 activity (Fig. 6C and D). Caspase-3 activity was enhanced by up to ~40% in the mutant-infected cells at 50 h post-infection, whereas that of WT and Mock treatment was increased by only ~5 and 2%, respectively. To evaluate the progency virus production from infected cells, virus titres in the culture supernatants at 24 and 50 h post-infection were investigated by focus-forming assay. There was no difference in progency virus production between the mutant and WT (Fig. 6E). It is known that WT does not have the ability for plaque formation, but the mutant was able to form plaques (Fig. 6F). In order to determine whether the cytotoxicity of infected cells was induced by cell–cell fusion, LLC-MK2 cells were co-transfected with the WT HN and each F gene, the WT and E170G, and then stained by DAPI, PI and the caspase-3 substrate. DNA condensation, cell death and caspase-3 activity were detected in syncytial cells that had been formed by cells transfected with E170G F gene (Fig. 6G). To investigate whether caspase-3 activation precedes or follows cell–cell fusion, we treated the transfected LLC-MK2 cells with a pan-caspase inhibitor, Z-VAD-FMK. Syncytium formation was not hampered by treatment with Z-VAD-FMK despite inhibition of caspase-3 activation (data not shown), suggesting that the enhanced fusion activity was not linked to downstream of caspase cascades.

We had isolated another mutant virus from the culture media after 12 serial passages. The virus had acquired a single mutation of Ala to Glu at amino acid position 442 in F glycoprotein. Unfortunately, the mutant virus showed slight reduction of viral sialidase activity and replication ability but had no obvious plaque formation, syncytium formation and caspase-3-dependent cell death abilities (data not shown). We tried to isolate other mutant viruses from the culture media, but we could not obtain any viruses that had acquired mutations in HN glycoprotein.

## Discussion

We demonstrated that a mutant virus isolated in the presence of TCM-Neu5Ac2en possessed two amino acid mutations at positions 170 and 442 in F glycoprotein but no mutation in HN glycoprotein and showed markedly higher fusion activity than that of WT (Fig. 1). We also demonstrated that syncytium formation of the mutant virus was responsible for a single mutation of Glu to Gly at position 170 in F glycoprotein (Fig. 5). Some studies have shown that mutation of HN glycoprotein affects viral fusion activity and that both the stalk and globular head region of HN glycoprotein are involved in fusion promotion (*21*, *25*, *29–33*). On the other hand, the mutation position in HR1 of F glycoprotein that increases fusion activity has been reported in other paramyxoviruses such as Newcastle disease virus (*34*), Sendai virus (*35*) and Simian virus 5 (*36*). However, our study is the first report to show that one amino acid mutation of hPIV1 F glycoprotein obviously promoted fusion activity. Mutations of F glycoprotein that induce HN-independent syncytium formation have been reported in paramyxoviruses including Newcastle disease virus (*32*, *37*) and Simian virus 5 (*38*, *39*). In the present study, transfection with the F gene alone of WT or mutants could not induce syncytium formation in LLC-MK2 cells. This result indicated that induction of syncytium formation by mutation of F glycoprotein was dependent on its interaction with HN glycoprotein.

The sialidase activity (the $V_{max}$ value) of the mutant virus was lower than that of WT, however there was no difference in the receptor binding (the values of $K_d$ and $B_{max}$) between the two viruses (Tables II and III). These results suggest that mutation of F glycoprotein induces a structural change of the active site(s) for sialidase activity but not receptor binding of HN glycoprotein.

Mammalian cells possess four sialidases, NEU1, NEU2, NEU3 and NEU4, which differ in intracellular localization and substrate specificity. In recent studies, mammalian sialidases have been shown to play an important role in cell differentiation and signalling (*40–43*). Additionally, actin remodelling via a small GTPase, RhoA, has been shown to be required for cell–cell fusion of viruses that belong to the *Paramyxoviridae* family (*21*, *44*). RhoA interacts with RSV F glycoprotein and contributes to syncytium formation (*45*). Therefore, the mutant virus F glycoprotein may be associated with activation of RhoA-mediated signalling.

The sialidase of the mutant virus does not have resistance against TCM-Neu5Ac2en (Fig. 2A and B), but the mutant exhibited remarkable fusion activity (Fig. 1). As shown in Fig. 4B, the penetration rate of the mutant virus was obviously higher than that of WT

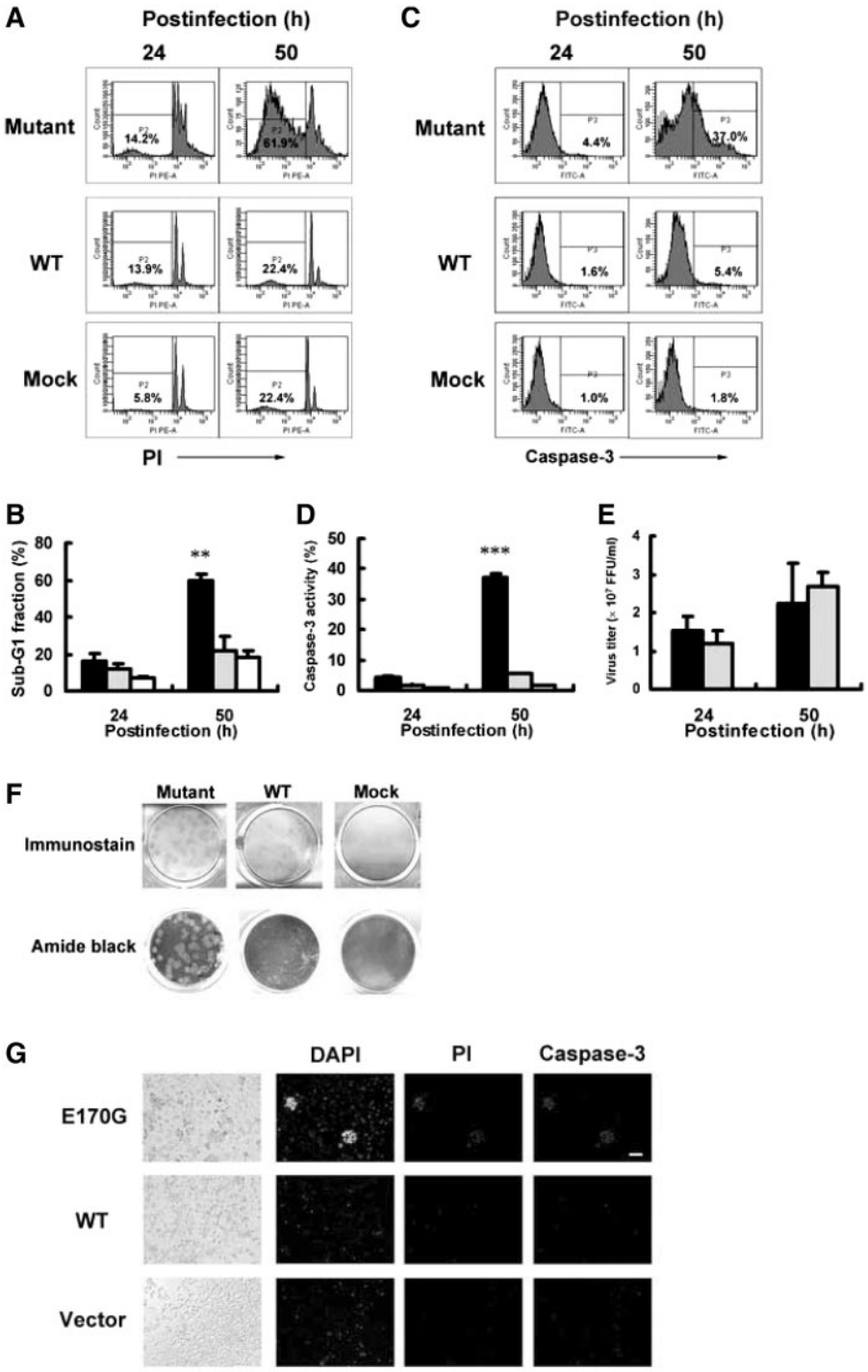


**Fig. 6 Induction of caspase-3-dependent cell death by mutant virus infection and by transfection with the F gene having a single amino acid change at position 170 (E170G).** LLC-MK2 cells were infected with each virus at m.o.i. of 4 and cultured in the presence of acetylated trypsin (1 μg/ml). Cell death (A) and caspase-3 activity (C) were measured at 24 and 50 h post-infection by PI staining and live Cells caspase-3 Assay Kit, respectively, as described in 'Materials and Methods' section. (B) Sub-G1 fraction of PI-stained cells was determined at 24 and 50 h post-infection. Sub-G1 fraction was calculated as a percentage of the cell number in the sub-G1 fraction within marker line P2 in (A) relative to that of all cells. (D) Caspase-3 activity of virus-infected cells was determined at 24 and 50 h post-infection. Caspase-3 activity fraction was calculated as a percentage of the cell number within the caspase-3-positive region within marker line P3 as in (C) relative to that of all cells. Mutant virus, closed column; WT, hatched column; Mock, open column. (E) LLC-MK2 cells were infected with each virus at m.o.i. of 4 and cultured in the presence of acetylated trypsin at 37°C. Progeny virus titers of the mutant virus (closed column) and WT (hatched column) in each supernatant at 24 and 50 h post-infection were measured by focus forming assay. (F) Viral foci were detected by immunostaining with rabbit anti-hPIV1 polyclonal antibody as previously described. Plaques were stained by 0.5% amide black solution. (G) LLC-MK2 cells co-transfected with HN and F gene (WT or E170G) were stained by DAPI, PI and caspase-3 substrate. As a negative control, pCAGGS/MCS vector was used instead of pCAGGS-F vector. Scale bar is 100 μm. $^{**}P<0.01$ and $^{***}P<0.001$.

at 7 and 15 min after infection. High penetration rate at the initial stage of viral infection and remarkable syncytium formation may enable the mutant virus to replicate efficiently in the presence of the sialidase inhibitor TCM-Neu5Ac2en.

The mutant virus showed much higher cytotoxicity than that of WT (Fig. 6A–D). Our results suggest that the cytotoxicity is induced by remarkable cell–cell fusion rather than the difference in viral production rate (Fig. 6E–G). In fact, caspase-3 activity was clearly detected in syncytial cells and was induced after cell–cell fusion in LLC-MK2 cells co-transfected with HN and E170G F genes (Fig. 6G). Besides, although both WT and the mutant virus showed viral focus by immunostaining, the mutant only formed clear viral plaque by inducing apoptosis (Fig. 6F). It has been reported that F glycoprotein of respiratory syncytial virus (RSV) triggered p53-dependent apoptosis (*46*). Increase in fusion activity of Sendai virus has been suggested to correlate with viral virulence *in vivo* (*47*). The mutant virus caused no cell–cell fusion and cytopathic effect without acetylated trypsin (data not shown). Therefore, the measured cytotoxicity of the mutant virus may be dependent on cell–cell fusion. The pre-fusion and post-fusion structures of fusion proteins in some viruses have been published (*26*, *48–52*), and two conflicting models of the fusion mechanism have been advocated (*53*). In the models, hPIV1 F glycoprotein is classified as a class I fusion protein, including influenza virus haemagglutinin glycoprotein of the *Orthomyxoviridae* family, human immunodeficiency virus (HIV) gp41 of the *Retroviridae* family and other F glycopoteins of the *Paramyxoviridae* family. One of the most important characteristics of class I fusion proteins are that HR1 and HR2 form 6HB for syncytium formation. The present findings therefore suggest that F glycoprotein plays a critical role in higher levels of replication, plaque formation and virus-induced cell death.

## Acknowledgements

This work was supported by the Global COE Program from the Japan Society for the Promotion of Science.

## Supplementary Data

Supplementary Data are available at *JB* Online.

## References

1. Suzuki, T., Portner, A., Scroggs, R.A., Uchikawa, M., Koyama, N., Matsuo, K., Suzuki, Y., and Takimoto, T. (2001) Receptor specificities of human respiroviruses. *J. Virol.* **75**, 4604–4613
2. Newman, J.T., Riggs, J.M., Surman, S.R., McAuliffe, J.M., Mulaikal, T.A., Collins, P.L., Murphy, B.R., and Skiadopoulos, M.H. (2004) Generation of recombinant human parainfluenza virus type 1 vaccine candidates by importation of temperature-sensitive and attenuating mutations from heterologous paramyxoviruses. *J. Virol.* **78**, 2017–2028
3. Fry, A.M., Curns, A.T., Harbour, K., Hutwagner, L., Holman, R.C., and Anderson, L.J. (2006) Seasonal trends of human parainfluenza viral infections: United States, 1990-2004. *Clin. Infect. Dis.* **43**, 1016–1022
4. Lucas, J.R., Haas, E.A., Masoumi, H., and Krous, H.F. (2009) Sudden death in a toddler with laryngotracheitis caused by human parainfluenza virus-1. *Pediatr. Dev. Pathol.* **12**, 165–168
5. Slobod, K.S., Shenep, J.L., Lujan-Zilbermann, J., Allison, K., Brown, B., Scroggs, R.A., Portner, A., Coleclough, C., and Hurwitz, J.L. (2004) Safety and immunogenicity of intranasal murine parainfluenza virus type 1 (Sendai virus) in healthy human adults. *Vaccine* **22**, 3182–3186
6. Skiadopoulos, M.H., Tatem, J.M., Surman, S.R., Mitcho, Y., Wu, S.L., Elkins, W.R., and Murphy, B.R. (2002) The recombinant chimeric human parainfluenza virus type 1 vaccine candidate, rHPIV3-1cp45, is attenuated, immunogenic, and protective in African green monkeys. *Vaccine* **20**, 1846–1852
7. Bartlett, E.J., Cruz, A.M., Boonyaratanakornkit, J., Esker, J., Castano, A., Skiadopoulos, M.H., Collins, P.L., Murphy, B.R., and Schmidt, A.C. (2010) A novel human parainfluenza virus type 1 (HPIV1) with separated P and C genes is useful for generating C gene mutants for evaluation as live-attenuated virus vaccine candidates. *Vaccine* **28**, 767–779
8. Zhan, X., Slobod, K.S., Krishnamurthy, S., Luque, L.E., Takimoto, T., Jones, B., Surman, S., Russell, C.J., Portner, A., and Hurwitz, J.L. (2008) Sendai virus recombinant vaccine expressing hPIV-3 HN or F elicits protective immunity and combines with a second recombinant to prevent hPIV-1, hPIV-3 and RSV infections. *Vaccine* **26**, 3480–3488
9. Jones, B., Zhan, X., Mishin, V., Slobod, K.S., Surman, S., Russell, C.J., Portner, A., and Hurwitz, J.L. (2009) Human PIV-2 recombinant Sendai virus (rSeV) elicits durable immunity and combines with two additional rSeVs to protect against hPIV-1, hPIV-2, hPIV-3, and RSV. *Vaccine* **27**, 1848–1857
10. Suzuki, T., Ikeda, K., Koyama, N., Hosokawa, C., Kogure, T., Takahashi, T., Hidari, K.I., Miyamoto, D., Tanaka, K., and Suzuki, Y. (2001) Inhibition of human parainfluenza virus type 1 sialidase by analogs of 2-deoxy-2,3-didehydro-*N*-acetylneuraminic acid. *Glycoconj. J.* **18**, 331–337
11. Ikeda, K., Sato, K., Nishino, R., Aoyama, S., Suzuki, T., and Sato, M. (2008) 2-Deoxy-2,3-didehydro-*N*-acetylneuraminic acid analogs structurally modified by thiocarbamoylalkyl groups at the C-4 position: Synthesis and biological evaluation as inhibitors of human parainfluenza virus type 1. *Bioorg. Med. Chem.* **16**, 6783–6788
12. Hu, X.L., Ray, R., and Compans, R.W. (1992) Functional interactions between the fusion protein and hemagglutinin-neuraminidase of human parainfluenza viruses. *J. Virol.* **66**, 1528–1534
13. Horvath, C.M., Paterson, R.G., Shaughnessy, M.A., Wood, R., and Lamb, R.A. (1992) Biological activity of paramyxovirus fusion proteins: factors influencing formation of syncytia. *J. Virol.* **66**, 4564–4569
14. Bagai, S. and Lamb, R. (1995) Quantitative measurement of paramyxovirus fusion: differences in requirements of glycoproteins between simian virus 5 and human parainfluenza virus 3 or Newcastle disease virus. *J. Virol.* **69**, 6712–6719
15. Sergel, T., McGinnes, L.W., Peeples, M.E., and Morrison, T.G. (1993) The attachment function of the Newcastle disease virus hemagglutinin-neuraminidase protein can be separated from fusion promotion by mutation. *Virology* **193**, 717–726

16. Moscona, A. (2005) Entry of parainfluenza virus into cells as a target for interrupting childhood respiratory disease. *J. Clin. Invest.* **115**, 1688–1698
17. Takimoto, T., Taylor, G.L., Connaris, H.C., Crennell, S.J., and Portner, A. (2002) Role of the hemagglutinin-neuraminidase protein in the mechanism of paramyxovirus-cell membrane fusion. *J. Virol.* **76**, 13028–13033
18. Ivanovic, T., Agosto, M.A., Zhang, L., Chandran, K., Harrison, S.C., and Nibert, M.L. (2008) Peptides released from reovirus outer capsid form membrane pores that recruit virus particles. *EMBO J.* **27**, 1289–1298
19. Matrosovich, M., Matrosovich, T., Garten, W., and Klenk, H.D. (2006) New low-viscosity overlay medium for viral plaque assays. *Virol. J.* **3**, 63
20. Suzuki, T., Sometani, A., Yamazaki, Y., Horiike, G., Mizutani, Y., Masuda, H., Yamada, M., Tahara, H., Xu, G., Miyamoto, D., Oku, N., Okada, S., Kiso, M., Hasegawa, A., Ito, T., Kawaoka, Y., and Suzuki, Y. (1996) Sulphatide binds to human and animal influenza A viruses, and inhibits the viral infection. *Biochem. J.* **318**, 389–393
21. Tsurudome, M., Nishio, M., Ito, M., Tanahashi, S., Kawano, M., Komada, H., and Ito, Y. (2008) Effects of hemagglutinin-neuraminidase protein mutations on cell-cell fusion mediated by human parainfluenza type 2 virus. *J. Virol.* **82**, 8283–8295
22. Suzuki, T., Jyono, M., Tsukimoto, M., Hamaoka, A., and Suzuki, Y. (1995) Labeling of influenza virus with alkylamine-modified horseradish peroxidase. *Anal. Biochem.* **228**, 42–47
23. Merz, D.C. and Wolinsky, J.S. (1981) Biochemical features of mumps virus neuraminidases and their relationship with pathogenicity. *Virology* **114**, 218–227
24. Waxham, M.N. and Aronowski, J. (1988) Identification of amino acids involved in the sialidase activity of the mumps virus hemagglutinin-neuraminadase protein. *Virology* **167**, 226–232
25. Huberman, K., Peluso, R.W., and Moscona, A. (1995) Hemagglutinin-neuraminidase of human parainfluenza 3: role of the neuraminidase in the viral life cycle. *Virology* **214**, 294–300
26. Bousse, T., Takimoto, T., Gorman, L.W., Takahashi, T., and Portner, A. (1994) Regions on the hemagglutinin-neuraminidase proteins of human parainfluenza virus type-1 and Sendai virus important for membrane fusion. *Virology* **204**, 506–514
27. Yin, H.S., Paterson, R.G., Wen, X., Lamb, R.A., and Jardetzky, T.S. (2005) Structure of the uncleaved ectodomain of the paramyxovirus (hPIV3) fusion protein. *Proc. Natl. Acad. Sci. USA* **102**, 9288–9293
28. Lee, J.K., Prussia, A., Paal, T, White, L.K, Snyder, J.P., and Plemper, R.K. (2008) Functional interaction between paramyxovirus fusion and attachment proteins. *J. Biol. Chem.* **283**, 16561–16572
29. Tsurudome, M., Kawano, M., Yuasa, T., Tabata, N., Nishio, M., Komada, H., and Ito, Y. (1995) Identification of regions on the hemagglutinin-neuraminidase protein of human parainfluenza virus type 2 important for promoting cell fusion. *Virology* **213**, 190–203
30. Deng, R., Wang, Z., Mirza, A.M., and Iorio, R.M. (1995) Localization of a domain on the paramyxovirus attachment protein required for the promotion of cellular fusion by its homologous fusion protein spike. *Virology* **209**, 457–469
31. Gravel, K.A. and Morrison, T.G. (2003) Interacting domains of the HN and F proteins of newcastle disease virus. *J. Virol.* **77**, 11040–11049
32. Tanabayashi, K. and Compans, R.W. (1996) Functional interaction of paramyxovirus glycoproteins: identification of a domain in Sendai virus HN which promotes cell fusion. *J. Virol.* **70**, 6112–6118
33. Bousse, T., Takimoto, T., and Portner, A. (1995) A single amino acid changes enhances the fusion promotion activity of human parainfluenza virus type 1 hemagglutinin-neuraminidase glycoprotein. *Virology* **209**, 654–657
34. Ayllón, J., Villar, E., and Muñoz-Barroso, I. (2009) Mutations in the ectodomain of the Newcastle Disease Virus Fusion protein confers hemagglutinin-neuraminidase independent phenotype. *J. Virol.* **84**, 1066–1075
35. Luque, L.E. and Russell, C.J. (2007) Spring-loaded heptad repeat residues regulate the expression and activation of paramyxovirus fusion protein. *J. Virol.* **81**, 3130–3141
36. West, D.S., Sheehan, M.S., Segeleon, P.K., and Dutch, R.E. (2005) Role of the simian virus 5 fusion protein N-terminal coiled-coil domain in folding and promotion of membrane fusion. *J. Virol.* **79**, 1543–1551
37. Li, J., Melanson, V.R., Mirza, A.M., and Iorio, R.M. (2005) Decreased dependence on receptor recognition for the fusion promotion activity of L289A-mutated newcastle disease virus fusion protein correlates with a monoclonal antibody-detected conformational change. *J. Virol.* **79**, 1180–1190
38. Ito, M., Nishio, M., Kawano, M., Kusagawa, S., Komada, H., Ito, Y., and Tsurudome, M. (1997) Role of a single amino acid at the amino terminus of the simian virus 5 F2 subunit in syncytium formation. *J. Virol.* **71**, 9855–9858
39. Paterson, R.G., Russell, C.J., and Lamb, R.A. (2000) Fusion protein of the paramyxovirus SV5: destabilizing and stabilizing mutants of fusion activation. *Virology* **270**, 17–30
40. Anastasia, L., Papini, N., Colazzo, F., Palazzolo, G., Tringali, C., Dileo, L., Piccoli, M., Conforti, E., Sitzia, C., Monti, E., Sampaolesi, M., Tettamanti, G., and Venerando, B. (2008) NEU3 sialidase strictly modulates GM3 levels in skeletal myoblasts C2C12 thus favoring their differentiation and protecting them from apoptosis. *J. Biol. Chem.* **283**, 36265–36271
41. Sato, K. and Miyagi, T. (1996) Involvement of an endogenous sialidase in skeletal muscle cell differentiation. *Biochem. Biophys. Res. Commun.* **221**, 826–830
42. Fanzani, A., Giuliani, R., Colombo, F., Zizioli, D., Presta, M., Preti, A., and Marchesini, S. (2003) Overexpression of cytosolic sialidase Neu2 induces myoblast differentiation in C2C12 cells. *FEBS Lett.* **547**, 183–188
43. Champigny, M.J., Perry, R., Rudnicki, M., and Igdoura, S.A. (2005) Overexpression of MyoD-inducible lysosomal sialidase (neu1) inhibits myogenesis in C2C12 cells. *Exp. Cell Res.* **311**, 157–166
44. Gower, T.L., Pastey, M.K., Peeples, M.E., Collins, P.L., McCurdy, L.H., Hart, T.K., Guth, A., Johnson, T.R., and Graham, B.S. (2005) RhoA signaling is required for respiratory syncytial virus-induced syncytium formation and filamentous virion morphology. *J. Virol.* **79**, 5326–5336
45. Pastey, M.K., Crowe, J.E. Jr, and Graham, B.S. (1999) RhoA interacts with the fusion glycoprotein of respiratory syncytial virus and facilitates virus-induced syncytium formation. *J. Virol.* **73**, 7262–7270

46. Eckardt-Michel, J., Lorek, M., Baxmann, D., Grunwald, T., Keil, G.M., and Zimmer, G. (2008) The fusion protein of respiratory syncytial virus triggers p53--dependent apoptosis. *J. Virol.* **82**, 3236–3249
47. Luque, L.E., Bridges, O.A., Mason, J.N., Boyd, K.L., Portner, A., and Russell, C.J. (2009) Residues in the heptad repeat a region of the fusion protein modulate the virulence of Sendai virus in mice. *J. Virol.* **84**, 810–821
48. Bullough, P.A., Hughson, F.M., Skehel, J.J., and Wiley, D.C. (1994) Structure of influenza haemagglutinin at the pH of membrane fusion. *Nature* **371**, 37–43
49. Chen, J., Skehel, J.J., and Wiley, D.C. (1999) N- and C-terminal residues combine in the fusion-pH influenza hemagglutinin HA (2) subunit to form an N cap that terminates the triple-stranded coiled coil. *Proc. Natl. Acad. Sci. USA* **96**, 8967–8972
50. Chen, L., Gorman, J.J., McKimm-Breschkin, J., Lawrence, L.J., Tulloch, P.A., Smith, B.J., Colman, P.M., and Lawrence, M.C. (2001) The structure of the fusion glycoprotein of Newcastle disease virus suggests a novel paradigm for the molecular mechanism of membrane fusion. *Structure* **9**, 255–266
51. Wilson, I.A., Skehel, J.J., and Wiley, D.C. (1981) Structure of the haemagglutinin membrane glycoprotein of influenza virus at 3 A resolution. *Nature* **289**, 366–373
52. Yin, H.S., Wen, X., Paterson, R.G., Lamb, R.A., and Jardetzky, T.S. (2006) Structure of the parainfluenza virus 5 F protein in its metastable, prefusion conformation. *Nature* **439**, 38–44
53. Connolly, S.A., Leser, G.P., Jardetzky, T.S., and Lamb, R.A. (2009) Bimolecular complementation of paramyxovirus fusion (F) and hemagglutinin-neuraminidase (HN) proteins enhances fusion: implications for the mechanism of fusion triggering. *J. Virol.* **83**, 10857–10868